G. Vanhoutte, N.R. Brooks, S. Schaltin, B. Opperdoes, L. Van Meervelt, J.P. Locquet, P.M. Vereecken, J. Fransaer, K. Binnemans
Journal of Physical Chemistry C 118, 20152–20162 (2014).

Electrodeposition of Lithium from Lithium-Containing Solvate Ionic Liquids

Gijs Vanhoutte,[†] Neil R. Brooks,[‡] Stijn Schaltin,[†] Bastiaan Opperdoes,[¶] Luc Van Meervelt,[‡] Jean-Pierre Locquet,[¶] Philippe M. Vereecken,[§] Jan Fransaer,[†] and Koen Binnemans[*,‡]

Department of Materials Engineering, KU Leuven, Kasteelpark Arenberg 44, B-3001 Leuven, Belgium, Department of Chemistry, KU Leuven, Celestijnenlaan 200F, B-3001 Leuven, Belgium, Department of Physics and Astronomy, KU Leuven, Celestijnenlaan 200D, B-3001 Leuven, Belgium, and Imec, Kapeldreef 75, B-3001 Leuven, Belgium

E-mail: Koen.Binnemans@chem.kuleuven.be

Phone: +32 (0)1632 7446. Fax: +32 (0)1632 7992

[*]To whom correspondence should be addressed
[†]Department of Materials Engineering, KU Leuven, Kasteelpark Arenberg 44, B-3001 Leuven, Belgium
[‡]Department of Chemistry, KU Leuven, Celestijnenlaan 200F, B-3001 Leuven, Belgium
[¶]Department of Physics and Astronomy, KU Leuven, Celestijnenlaan 200D, B-3001 Leuven, Belgium
[§]Imec, Kapeldreef 75, B-3001 Leuven, Belgium

Abstract

Lithium-containing solvate ionic liquids $[Li(L)_n][X]$ with ligands L = 1,2-dimethoxyethane (G1, monoglyme) or 1-methoxy-2-(2-methoxyethyl)ether (G2, diglyme) (with n = 1, 2 or 3) and with anions X = bis(trifluoromethylsulfonyl)imide (Tf_2N^-), bromide (Br^-) or iodide (I^-) were synthesized and used as electrolytes for the electrodeposition of lithium metal. Very high lithium-ion concentrations could be obtained, since the lithium ion is part of the cationic structure of the solvate ionic liquids. Without stirring, current densities up to -26 A dm^{-2} at a potential of -0.5 V vs. Li/Li^+ were registered during cyclic voltammetry. The formation of a solid-electrolyte interface during electrodeposition of lithium from $[Li(G1)_2][Tf_2N]$ was studied by electrochemical quartz microbalance and Auger electron spectroscopy. SEM pictures revealed uniform and nondendritic lithium deposits.

Keywords

Auger electron spectroscopy; electrochemical quartz microbalance; electrodeposition; ionic liquids; lithium; rechargeable batteries; solid-electrolyte interface

Introduction

The high specific energy density of lithium batteries makes them attractive as power sources for a wide range of applications.[1] Concerns about the safety associated with the electrolytes based on volatile organic solvents have necessitated the use of lithium intercalation materials (rather than lithium metal) as anodes, which decreases the energy storage capacity per unit mass.[2] Room-temperature ionic liquids (RTILs), which are solvents that consist entirely of cations and anions, have attracted quite a lot of attention owing to their unique properties such as low volatility, high thermal stability, high ionic conductivity, wide electrochemical window and high chemical stability.[3–6]

Even though ionic liquids could improve the safety of lithium metal batteries, other challenges have to be overcome before lithium metal can be used as an anode material in batteries. Two major challenges are the suppression of dendrite formation[7–10] and the formation of a stable solid-electrolyte interface (SEI).[8,11–13] These two properties affects the lifetime and safety of lithium batteries. In general, the approaches to overcome these challenges include the use of additives which improve the plating morphology[14–17] and the use of polymer electrolytes.[18–20] Also ionic liquids have proven to be useful as electrolytes for secondary lithium batteries with high cycling efficiencies[7,21–23] and they were even tested in a battery prototype by Kim et al.[24] Due to their wide thermal stability window, ionic liquids can even be used as electrolytes for high-temperature lithium batteries.[25]

Nevertheless, no electrolytes have been found which are stable against the reducing power of lithium, which results in a layer of decomposition products at the lithium-electrolyte interface. A so called solid-electrolyte interface (SEI) is formed on the interface between lithium and the electrolyte, because lithium is thermodynamically unstable in contact with many solvents and salts.[26] The formation of a good SEI is a major challenge when new electrolytes for lithium batteries are tested.[10,21] Especially the characterization of the SEI is not an easy task. According to Howlett *et al.* they were the first in 2006 to describe the composition and structure of the SEI formed on lithium depositions made from the ionic liquid, *N*-methyl-*N*-alkylpyrrolidinium bis(trifluoromethylsulfonyl)imide.[12]

Mixtures of oligoethers or glymes, $CH_3(CH_2CH_2O)_nCH_3$, with lithium salts have been widely studied as models of poly(ethylene oxide)-based polymer electrolytes for lithium-ion batteries.[27–30] It was found that various chain lengths of glymes could be used to form structurally well-defined complexes with melting points below 100 °C.[31–36] Ueno et al. have shown that these [Li(glyme)][X] complexes act as ionic liquids, rather than concentrated organic solutions, based on the competitive interactions between glymes and counter anions and between glymes and lithium ions.[37] According to Angell et al., ionic liquids can be categorized into four groups: aprotic, protic, inorganic and solvate (or chelate) ionic liquids.[38]

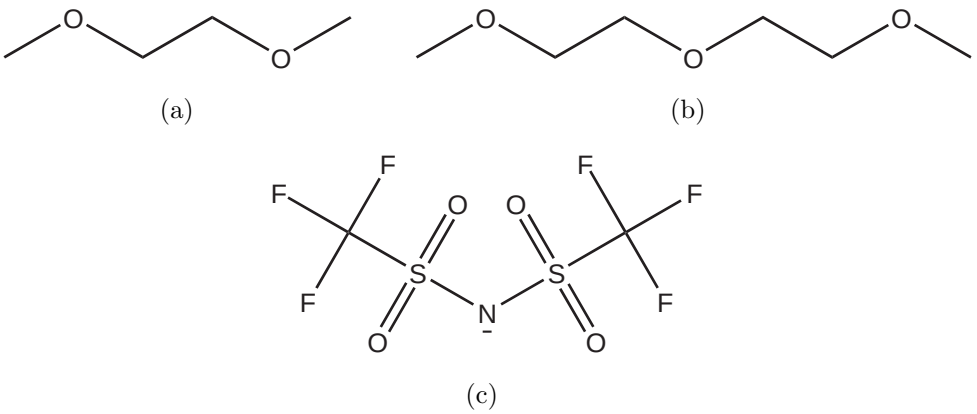

Figure 1: Structural formula of the used ligands and anion: (a) monoglyme (G1), (b) diglyme (G2) and (c) bis(trifluoromethylsulfonyl)imide (Tf_2N^-).

In "solvate" ionic liquids, ligand molecules coordinate strongly to the cation of the metal salts, thereby forming complex ions. Recently, Mandai *et al.* summarized possible criteria for classifying solutions as solvate ionic liquids.[39] Since the metal cation is an intrinsic part of the cationic structure of the ionic liquid, high metal concentrations can be obtained in these metal-containing ionic liquids.[40–43] Such metal-containing ionic liquids proved to be interesting electrolytes for high-rate electrodeposition of metals. The concept of high-rate electrodeposition from metal-containing ionic liquids has already been reported for copper- and silver-containing ionic liquids, where electrodeposition was possible at current densities larger than -25 A dm^{-2}.[44–49]

In this paper, we report on solvate ionic liquids $[Li(L)_n][X]$ with a lithium-containing cation, formed by coordination of the ligand L = 1,2-dimethoxyethane (G1, monoglyme) or 1-methoxy-2-(2-methoxyethyl)ether (G2, diglyme) (n = 1, 2 or 3) to a lithium ion (Figure 1). As anion (X), either bis(trifluoromethylsulfonyl)imide (Tf_2N^-), bromide or iodide were used. These lithium-containing solvate ionic liquids were investigated as electrolytes for lithium metal deposition and the electrochemical behavior was compared. $[Li(G1)_2][Tf_2N]$ was selected for a more detailed study as electrolyte for lithium metal deposition and studied by means of cyclic voltammetry, electrochemical quartz crystal microbalance (EQCM), scanning electron microscopy (SEM) and Auger electron spectroscopy (AES).

Results and discussion

Synthesis and characterization

Solvate ionic liquids, with the general formula $[Li(L)_n][X]$ (with L = G1 or G2, n = 1, 2 or 3 and X = Tf_2N^-, Br^- or I^-) were prepared by stoichiometric addition of the ligands to the lithium salts without the use of an additional solvent and at elevated temperatures, the lithium-containing ionic liquids were formed. Watanabe et al. focused on lithium based solvate ionic liquids. They successfully improved the stability and properties of this new class of ionic liquids by using multidendate ligands and concluded that triglyme (G3) and tetraglyme (G4) ligands result in the most stable cationic complex, although shorter glyme chains can also be used as ligands in solvate ionic liquids.[43] Lithium-glyme complexes have also extensively been studied by Henderson et al.[32] Phase diagrams and crystal structures were used to gain insight into the molecular interactions in these glyme-salt mixtures.[31] Recently possible criteria were summarized to classify liquids as solvate ionic liquids:[39]

1. Form a solvate compound between an ion and a ligand(s) in a certain stoichiometric ratio.

2. Consist entirely of complex ions (solvates) and their counter ions in the molten state.

3. Show no physicochemical properties based on both pure ligands and precursor salts under using conditions.

4. Have a melting point below 100 °C, which satisfies the criterion for typical ionic liquids.

5. Have a negligible vapor pressure under typical application conditions.

In order to meet all these criteria, various techniques were used to conclude that solvate ionic liquids were obtained. Based on crystal structures reported in literature[31,33,34,36] and the new crystal structure here presented (vide infra), it is clear that there is a strong interaction between ion and ligands when mixed in a stoichiometric ratio. These results were supported

by Raman spectroscopy, where a band at 870–890 cm^{-1} was observed, corresponding to the complexation of the glymes with the lithium cation, which is absent in pure glymes (See supporting information).[39] From thermogravimetric results obtained by Zhang et al. it can be seen that complexes with monoglyme (G1) and diglyme (G2) ligands result in a better thermal stability compared to the pure solvents.[43] From our own experience a better electrochemical stability was obtained for $[Li(G1)_2][Tf_2N]$ compared to the pure monoglyme. Where the oxidation of ether compounds start below 4 V vs. Li/Li^+, here an improved stability was observed with an anodic limit of approx. 4.9 V vs. Li/Li^+ for $[Li(G1)_2][Tf_2N]$.

All compounds had melting points below 100 °C (Table 1). Bis(trifluoromethylsulfonyl)-imide is commonly used as anion in ionic liquids to reduce the melting point of the ionic liquids. For the solvate ionic liquids with monoglyme ligands, the melting points decrease as a function of the anion in the order: $I^- > Br^- > Tf_2N^-$. For all anions, two monoglyme molecules per lithium cation resulted in the lowest melting point. When the lithium cation is coordinated by diglyme ligands, no clear trend in melting points is observed. The lowest melting points were measured when bromide anions were used. Unfortunately, these ionic liquids were very viscous preventing their study by electrochemical methods. The melting point depends on the interactions between the lithium cation and the ligand and/or the anion. The lithium cations tend to be fully solvated by the ether oxygens as solvent-separated ion pair (SSIPs) when enough ether oxygens (typically five or six) are present.[31,50–53] When fewer ether oxygens are present, a contact ion pair (CIP) or aggregate (AGG) solvates can be formed, where also the anion is coordinated to a lithium cation. These coordination complexes are also reflected in the crystal structures of the liquid lithium salts and are well described in literature.[31–34,36] For the crystalline solvates of $[Li(G1 \text{ or } G2)_x][Tf_2N]$, the coordination number of Li^+ is in the range of 4-6,[31] and excess glyme molecules exist in the electrolytes with $[O]/[Li^+] > 6$.[39] The reduced volatility of glymes for $[O]/[Li^+] > 6$ is explained simply by the vapor pressure depression due to the mixing of the solute and the solvent. For $[O]/[Li^+] < 6$, it is anticipated that free (uncoordinated) glyme molecules

Table 1: Melting points (°C) of compounds $[Li(G1)_n][X]$ and $[Li(G2)_n][X]$

	Tf_2N^-	Br^-	I^-
$[Li(G1)_1]^+$	62 (56)[Ref. 35]	–	–
$[Li(G1)_2]^+$	21 (20)[Ref. 31]	43	69
$[Li(G1)_3]^+$	29 (29)[Ref. 35]	45	71
$[Li(G2)_1]^+$	–	-33	58
$[Li(G2)_2]^+$	81 (83)[Ref. 35]	-8	78

scarcely exist in the $[Li(G1 \text{ or } G2)_x][Tf_2N]$ liquid.[39] A more concluding parameter to describe the stability of the complexes would be the complex formation constant, $K_{complex}$ or even better K_n (high-order complex formation constant, n = 1, 2, 3) unfortunately no reports addressing these constants are available for stoichiometric lithium-glyme mixtures.

For $[Li(G1)_3][I]$ and $[Li(G2)_2][I]$ it was possible to grow single crystals by slow cooling of the melt. The crystals were very hygroscopic and great care was required to mount them on the diffractometer. The structure of $[Li(G2)_2][I]$ was found to consist of discrete $[Li(G2)_2]^+$ cations, where the lithium centers are coordinated by six ether oxygens from the two G2 molecules, and discrete iodide anions (Figure 2). Single crystals of $[Li(G1)_3][I]$ were also studied and found to crystallize in the orthorhombic crystal system with the unit cell dimensions: $a = 12.0523(5)$ Å, $b = 7.3239(4)$ Å and $c = 10.1919(9)$ Å. However, in the structure refinement it was found that the G1 ligands were highly disordered and despite great attempts to find a satisfactory disorder model it was not possible to bring it to a publishable standard. It appears, however, that the structure consists of discrete $[Li(G1)_3]^+$ cations and iodide anions.

The crystal structures $[Li(G1)_1][Tf_2N]$,[36] $[Li(G2)_1][Tf_2N]$,[31] $[Li(G2)_2][Tf_2N]$,[31] $[Li(G1)_2][Br]$[33] and $[Li(G1)_2][I]$[34] have been previously reported. The structures of $[Li(G1)_1][Tf_2N]$[36] and $[Li(G2)_1][Tf_2N]$[31] were found to be polymeric in the solid state, whilst $[Li(G2)_2][Tf_2N]$[31] was found to consist of discrete $[Li(G2)_2]^+$ cations and Tf_2N^- anions. The structures of $[Li(G1)_2][Br]$[33] and $[Li(G1)_2][I]$[34] were found to consist of neutral discrete molecules in the solid state where the two G1 ligands and the halide anion are coordinated to the lithium

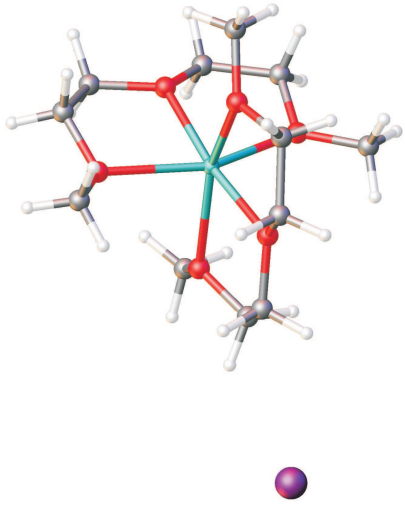

Figure 2: View of the crystal structure of $[Li(G2)_2][I]$ showing the cation and anion pair (disorder not shown for clarity). Color codes: C (gray), H (white), I (purple), Li (cyan), O (red).

Table 2: Viscosity η (mPa s) and conductivity (Ω^{-1} m^{-1}) of $[Li(G1)_2][Tf_2N]$

Temperature (°C)	Viscosity (mPa s)	Conductivity (Ω^{-1} m^{-1})
30	25	0.46
40	18	0.63
50	15	0.81
60	12	0.98
70	10	1.2

center.

For $[Li(G1)_2][Tf_2N]$, which was selected for lithium deposition experiments (based on melting point and Coulombic efficiency data: *vide infra*), absolute viscosity and electrical conductivity were measured as a function of temperature (Table 2). These show that $[Li(G1)_2][Tf_2N]$ has a very low viscosity and a high electrical conductivity.

Comparative electrochemical study

It is known that the bis(trifluoromethylsulfonyl)imide anion is not stable in contact with metallic lithium.[10,12,13,21,54,55] These decomposition compounds leads to the formation of a solid-electrolyte interface, which acts as a passivation layer to prevent further decomposition of the electrolyte.[12,54,56] However an inherent stable electrolyte would overcome the need for a solid-electrolyte interface. Therefore bromide and iodide were selected as counter anions in the ionic liquids in the hope of avoiding chemical decomposition of the anion. It was also tried to prepare solvate ionic liquids with chloride anions via the same synthetic method as used for the synthesis of the bromide and iodide compounds, but this was unsuccessful and only starting products were found back after reaction. The use of halide anions should result in higher Coulombic efficiencies in comparison with bis(trifluoromethylsulfonyl)imide anions for the electrodeposition and dissolution process of lithium, since no lithium metal is lost due to decomposition of the anion, because bromide and iodide are already in their lowest oxidation state. The Coulombic efficiency is defined as the ratio between the amounts of the electric charge delivered during stripping to the charge consumed for the deposition of lithium.[57] The charges were calculated by integrating the current over time under the curves of the cylcic voltammogram. selection of solvate ionic liquids were chosen from those synthesized to compare their electrochemical behavior: $[Li(G1)_2][Tf_2N]$, $[Li(G1)_2][Br]$, $[Li(G2)_2][Br]$ and $[Li(G1)_3][I]$.

From the cyclic voltammograms of bromide and bis(trifluoromethylsulfonyl)imide containing ionic liquids, it can be seen that with $[Li(G1)_2][Tf_2N]$, higher current densities could be achieved than in the case of the bromide-based ionic liquids (Figure 3). For $[Li(G1)_2][Tf_2N]$, a reduction current density of approx. $-5.5\,A\,dm^{-2}$ was reached, whereas for $[Li(G1)_2][Br]$ the current density was only $-3.8\,A\,dm^{-2}$ at a potential of -0.5 V vs. Li/Li^+. The lowest reduction current density ($-2.8\,A\,dm^{-2}$) was measured for $[Li(G2)_2][Br]$. For the stripping of lithium, the order changed. $[Li(G1)_2][Tf_2N]$ still reached the highest oxidation current densities of approx. $+2.5\,A\,dm^{-2}$, but the peak current densities for $[Li(G1)_2][Br]$

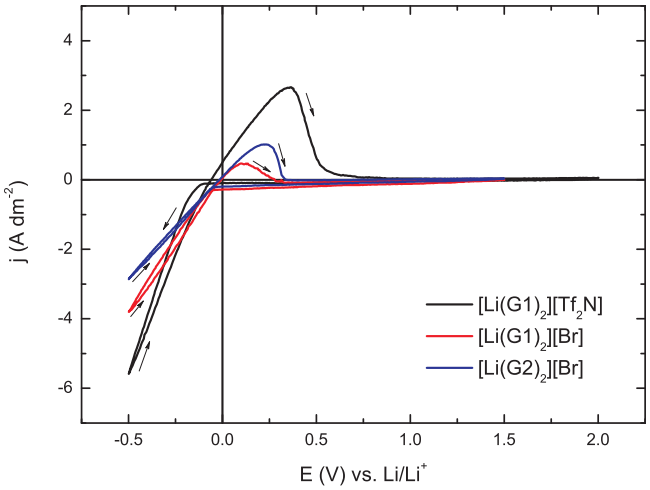

Figure 3: Cyclic voltammograms of liquid lithium salts with bromide and bis(trifluoromethylsulfonyl)imide anions. A copper working electrode ($\phi = 1$ mm) and a lithium counter and pseudo-reference electrode were used. The electrolyte was not stirred and a scan rate of $50\,\mathrm{mV\,s^{-1}}$ was applied. Three different electrolytes were tested: [Li(G1)$_2$][Tf$_2$N] (black), [Li(G1)$_2$][Br] (red) and [Li(G2)$_2$][Br] (blue) all at 70 °C.

were lower than for [Li(G2)$_2$][Br], with values of $+0.5\,\mathrm{A\,dm^{-2}}$ and $+1.0\,\mathrm{A\,dm^{-2}}$, respectively. These results show that changing the anion from bis(trifluoromethylsulfonyl)imide to bromide does not increase the Coulombic efficiency, as had been expected.

The cyclic voltammogram of [Li(G1)$_3$][I] was more promising because the slope of the reduction current density was much higher and a current density of $-6.0\,\mathrm{A\,dm^{-2}}$ could already be obtained at a potential of $-0.2\,\mathrm{V}$ vs. Li/Li$^+$ (Figure 4). In comparison, when [Li(G1)$_2$][Tf$_2$N] was used, a potential of $-0.5\,\mathrm{V}$ was needed to reach a similar reduction current density of $-5.5\,\mathrm{A\,dm^{-2}}$. Also the oxidation current density for [Li(G1)$_3$][I] reached a higher peak value ($+4\,\mathrm{A\,dm^{-2}}$), compared to the value of $+2.5\,\mathrm{A\,dm^{-2}}$ for Li(G1)$_2$][Tf$_2$N]. However, the oxidation peak for [Li(G1)$_2$][Tf$_2$N] is much broader compared to the peak of [Li(G1)$_3$][I] resulting in a higher charge during the stripping of the lithium metal.

The Coulombic efficiency for all the reduction-oxidation cycles was determined from the charge under the curves (Figure 5). To compare the performance of the different solvate ionic liquids, the Coulombic efficiency of the fifth cycle was considered. The highest Coulombic efficiency was observed for [Li(G1)$_2$][Tf$_2$N] with a value of 47 %. Using an iodide

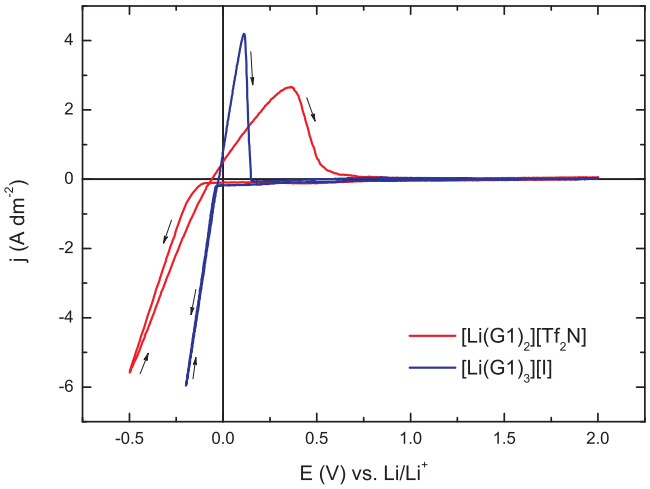

Figure 4: Cyclic voltammograms of liquid lithium salts with bromide and bis(trifluoromethylsulfonyl)imide anions. A copper working electrode (ϕ = 1 mm) and a lithium counter and pseudo-reference electrode were used. The electrolyte was not stirred and a scan rate of 50 mV s^{-1} was applied. Two different electrolytes were tested: $[Li(G1)_2][Tf_2N]$ (red) and $[Li(G1)_3][I]$ (blue) both at 70 °C.

anion as counter ion, the Coulombic efficiency for $[Li(G1)_3][I]$ reached 26 % after five cycles. The Coulombic efficiency using a bromide anion was 12 % and 9 % for $[Li(G2)_2][Br]$ and $[Li(G1)_2][Br]$, respectively.

From these results it can be concluded that also the ligands G1 and G2 were not stable against lithium metal as was found by Aurbach et al.,[58] because the Coulombic efficiency in all systems was lower than 50 %. The higher Coulombic efficiency for the bis(trifluoromethylsulfonyl)imide anion suggests that the decomposition of bis(trifluoromethylsulfonyl)-imide anion results in a better performing solid-electrolyte interface, as suggested by Howlett et al.[21] Another reason for the low Coulombic efficiency for halide containing solvate ionic liquids could be a more dendritic morphology of the electrodeposited lithium.[21]

Deposition of lithium from $[Li(G1)_2][Tf_2N]$

$[Li(G1)_2][Tf_2N]$ was selected for a more detailed study of the electrodeposition of lithium from lithium-containing ionic liquids, because it has a low melting point (Table 1), low viscosity, high electrical conductivity (Table 2) and high Coulombic efficiency (Figure 5).

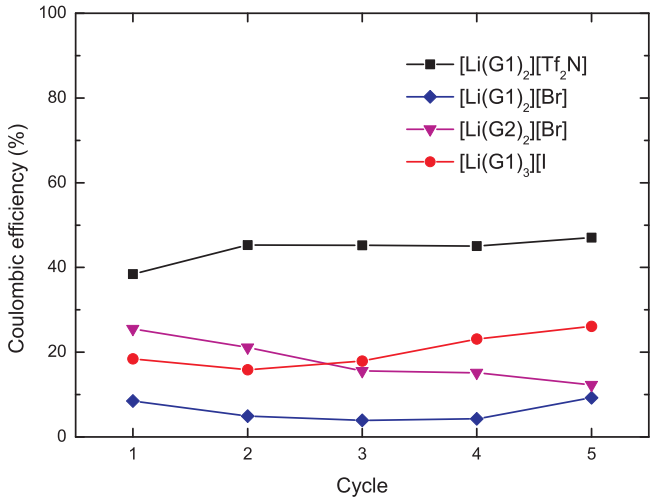

Figure 5: Coulombic efficiency calculated for reduction-oxidation cycles using four lithium-containing electrolytes: $[Li(G1)_2][Tf_2N]$ (black, ■), $[Li(G1)_2][Br]$ (blue, ♦), $[Li(G2)_2][Br]$ (magenta, ▼), $[Li(G1)_3][I]$ (red, •). Electrolytes were not stirred, at 70 °C and a scan rate of 50 mV s^{-1} was applied. A copper working electrode (ϕ = 1 mm), a lithium counter and pseudo-reference electrode was used.

The influence of different working electrode materials on the electrochemical reaction at the electrode surface was studied, because the reaction kinetics are controlled by the properties of the electrode-electrolyte interface. The effect on the formation of the solid-electrolyte interface was studied by comparing the Coulombic efficiency of the reduction-oxidation cycles on different electrodes. The working electrodes used in this study were platinum (ϕ = 0.5 mm), copper (ϕ = 1.0 mm) and titanium (ϕ = 2.0 mm). In all cases lithium was used as counter and pseudo-reference electrode, the electrolyte, $[Li(G1)_2][Tf_2N]$, was not stirred and kept at 70 °C. The potential was scanned with a scan rate of 50 mV s^{-1}.

The effect of different working electrodes on the reduction and oxidation behavior is very large (Figure 6). The highest reduction current density of -26 A dm^{-2} was observed when platinum was used. For a copper working electrode a current density of -5.5 A dm^{-2} was measured. The lowest reduction current density of -4.5 A dm^{-2} was measured for a titanium working electrode. All current densities were measured at a potential of -0.5 V vs. Li/Li^+.

Also during stripping, large differences were observed for various working electrode materials. When platinum was used, three oxidation peaks were observed, the highest with

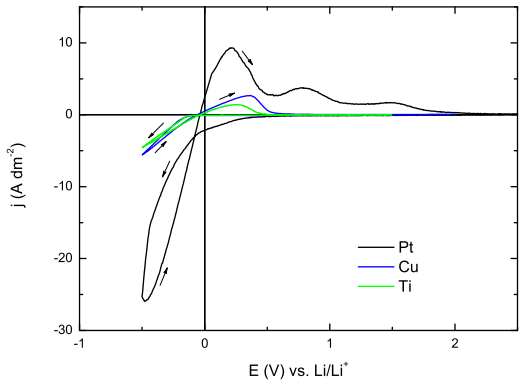

Figure 6: Third cycle of cyclic voltammograms using $[Li(G1)_2][Tf_2N]$ at 70 °C with various materials as working electrodes: platinum ($\phi = 0.5$ mm, black), copper ($\phi = 1.0$ mm, blue) and titanium ($\phi = 2.0$ mm, green). Lithium was used as pseudo-reference electrode and platinum as counter electrode. The electrolyte was not stirred and a scan rate of 50 mV s^{-1} was applied.

a peak current density of approx. +9 A dm^{-2} at +0.2 V vs. Li/Li$^+$, a second smaller peak of approx. +4 A dm^{-2} at +0.8 V vs. Li/Li$^+$ and the smallest peak of approx. +2 A dm^{-2} at +1.5 V vs. Li/Li$^+$. These extra oxidation peaks are the result of lithium-platinum alloy formation during deposition.[8]

Comparing the Coulombic efficiency of the reduction-oxidation cycles for different working electrodes it can be seen that the Coulombic efficiency increases with increasing cycle number for all working electrodes. However, in absolute numbers there is a big difference between the various materials. Comparing the Coulombic efficiency of the third cycle of the voltammograms, the lowest Coulombic efficiency of 23 % is found for the titanium electrode. The highest Coulombic efficiencies were observed for the copper and platinum electrodes with a Coulombic efficiency of 45 % and 50 %, respectively. It has been suggested that the lithium-platinum alloy formation provides a strong base for the solid-electrolyte interface, which explains the highest efficiency.[8] In a cycling study by Howlett et al. it was shown that the lithium metal cycling efficiency from *N*-methyl-*N*-alkylpyrrolidinium bis-(trifluoromethylsulfonyl)imide ionic liquids using a platinum working electrode could reach more than 99 %. Also in this study, initially a low efficiency was observed, but after cycle

10, the efficiency exceeded 95 %.[21]

A low Coulombic efficiency is mainly due to the reactivity of lithium metal and decomposition of the ionic liquid forming a solid-electrolyte interface during the first cycles. Another cause for a low efficiency is dendrite formation, these dendrites easily break during the stripping and are thereby disconnected from the electrode. This means that these pieces of lithium metal cannot be oxidized again when a positive current is applied, so that the Coulombic efficiency decreases with increasing dendrite formation. Platinum resulted in the highest efficiency, nevertheless copper was chosen as deposition substrate for a more detailed investigation, since copper is used as current collector in lithium-ion batteries and copper does not suffer from alloy formation as opposed to the platinum electrode.

Comparing cyclic voltammograms of $[Li(G1)_2][Tf_2N]$ at 30 °C when various scan rates were applied (Figure 7), it can be seen that both reduction and oxidation current densities do not depend on the scan rate. For the reduction, current density values of approx. $-2.2\,A\,dm^{-2}$ at -0.5 V vs. Li/Li^+ were measured for all scan rates ranging from $10\,mV\,s^{-1}$ to $100\,mV\,s^{-1}$. Therefore it can be concluded that the reduction of lithium ions in $[Li(G1)_2][Tf_2N]$ is kinetically controlled, instead of mass-transfer-controlled. Of course, if thick layers are deposited from $[Li(G1)_2][Tf_2N]$, it is possible that after a certain time the metal concentration decreases and the deposition becomes mass-transfer-controlled.

The decomposition of the electrolyte in contact with lithium metal is one possible reason for the poor Coulombic efficiency. This hypothesis was tested by measurements with an Electrochemical Quartz Crystal Microbalance (EQCM), which already proved its use for studying lithium deposition/dissolution from lithium-glyme solvate ionic liquids.[59] In the case of lithium, these results are relatively easy to interpret because lithium is one of the lightest elements in the periodic table. This means that when the mass increase is higher than expected based on calculations from charge data, other elements besides lithium contribute to this mass increase. The Coulombic efficiency was less than 100 %, which resulted in an incremental mass increase during subsequent cycles. The experimental mass increase

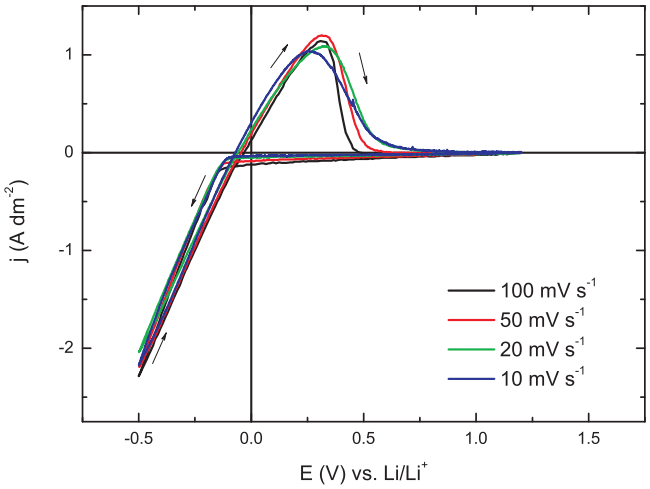

Figure 7: Cyclic voltammograms of $[Li(G1)_2][Tf_2N]$ at various scan rates. A copper working electrode ($\phi = 1\,\text{mm}$) and a platinum counter and a lithium pseudo-reference electrode were used. The electrolyte was not stirred and at a temperature of 30 °C.

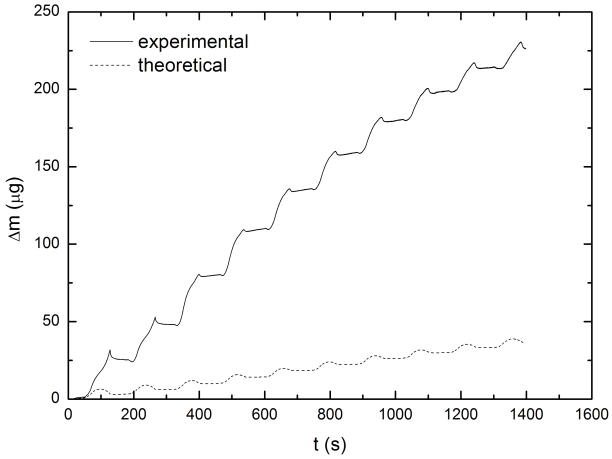

Figure 8: Mass changes during lithium deposition-dissolution on a copper substrate by EQCM, using $[Li(G1)_2][Tf_2N]$ as electrolyte at ambient temperature inside the glove box ($\approx 30\,°C$). A scan rate of $50\,\text{mV}\,\text{s}^{-1}$ was applied. A platinum counter electrode and a silver pseudo-reference electrode were used.

after ten cycles was about six times higher than the mass increase expected on the basis of theoretical calculations for lithium metal, that would remain on the electrode due to incomplete stripping (Figure 8). The magnitude of the mass increase during the first few cycles is different compared to the last cycles. Therefore a comparison was made between the first and after ten cycles (Figure 9). The mass increased when the current became negative,

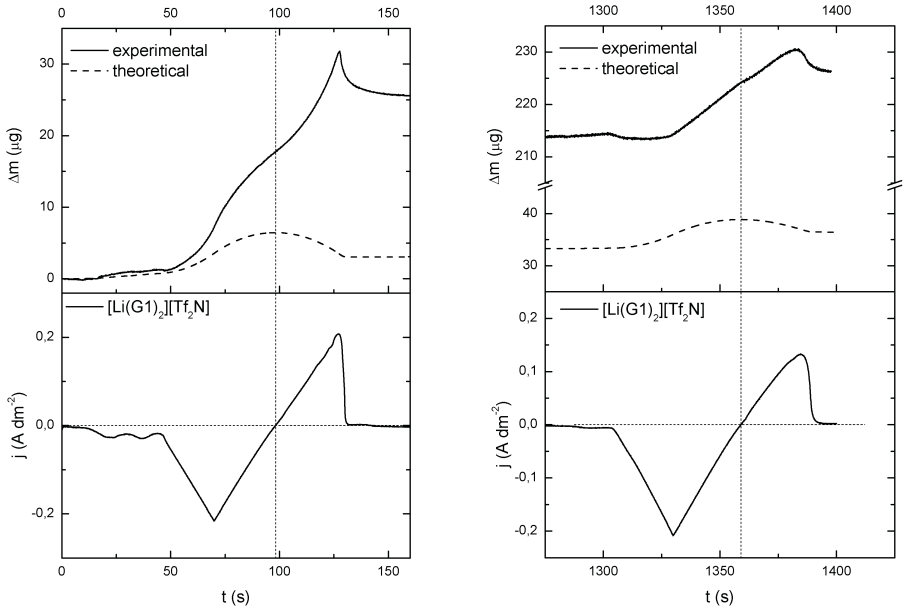

(a) cycle 1 (b) cycle 10

Figure 9: Comparison between theoretical mass change, current and experimental mass change (by EQCM) versus time for (a) cycle 1 and (b) cycle 10.

indicating that lithium was deposited onto the working electrode. After the vertex potential of $-4.5\,\mathrm{V}$ vs. Ag was reached, the scan was reversed and the current became less negative, but still lithium was being deposited on the substrate. From the total cathodic charge a mass increase of $6.5\,\mu\mathrm{g}$ was expected for lithium deposition only. However, a mass increase of $18\,\mu\mathrm{g}$ was found at the potential of zero current. A positive current indicates stripping of the electrodeposited lithium metal. The theoretical mass decreased by approx. $3\,\mu\mathrm{g}$, but actually the experimental mass kept increasing. After all the lithium was stripped from the working electrode and the current had fallen to zero, an experimental mass of approx. $25.5\,\mu\mathrm{g}$ was measured on the quartz crystal. The observation that the mass measured by the EQCM kept increasing at potential values where stripping of lithium is happening, is an indication that the electrolyte is not stable towards metallic lithium. The chemical reaction between metallic lithium and the electrolyte continued until all lithium deposited on the electrode had reacted or was stripped. Although the mass kept increasing through the stripping of lithium, only at the very end, just before the current dropped to zero there was a very small mass decrease

of 5 µg (Figure 9(a)). The theoretical mass after one deposition-stripping cycle, taking into account the Coulombic efficiency is 3 µg, however there was actually more than eight times this theoretical mass. This behavior changed, after the first cycle. Looking to the tenth and last cycle recorded the mass increase was more constant during deposition (Figure 9(b)). Again the mass kept increasing even during stripping of the lithium metal. After the tenth cycle the theoretical mass was about 36 µg and the experimental mass was approx. 226 µg, which is more than six times higher. The relative difference between the experimental and the theoretical mass after one cycle was 850 %, whereas for whole experiment this difference was 630 %. This means that during the first cycle more electrolyte reacts with metallic lithium, which is an indication that a more stable solid-electrolyte interface is formed during the experiment.

The morphology of the lithium deposits and the solid-electrolyte interface was studied by scanning electron microscopy (SEM). A potentiostatic electrodeposition was performed at a potential of −0.25 V vs. Li/Li^+ and stopped after a charge density of -224.5 C dm^2 was deposited. A layer of lithium with a theoretical thickness of 3 µm was deposited onto a copper wafer with a surface of about 49 mm^2 (7×7 mm). Deposits were made using $[Li(G1)_2][Tf_2N]$ as electrolyte at 30 °C and the solution was not stirred. SEM pictures reveal a rough, but well-covered surface (Figure 10). On the cross section, two layers could be distinguished: a dense layer of 2.2 to 3.4 µm thick and a second rough layer with maximum thicknesses of 10 µm. The deposits were rough, but not dendritic.

Decomposition of the ionic liquid in contact with metallic lithium and formation of the solid-electrolyte interface was studied by Auger Electron Spectroscopy (AES). Information obtained from AES is limited to the outer few atomic layers, so the depth profile was studied by etching the surface with argon ions. The surface was etched for eight min after each measurement and in total seven etch steps were performed thus the total etch time was 56 min. Five elements were detected: a LMM sulfur peak around 149 eV, a KLL carbon peak around 264 eV, a KLL nitrogen peak around 378 eV, three KLL oxygen peaks around

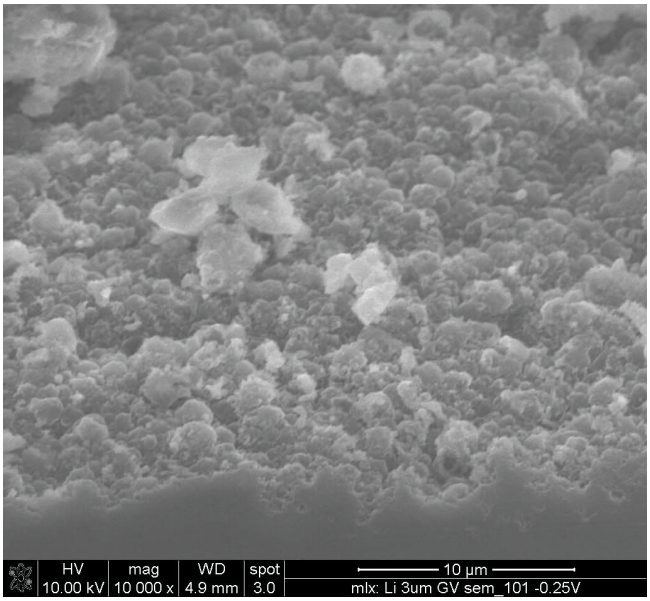

(a) Top view

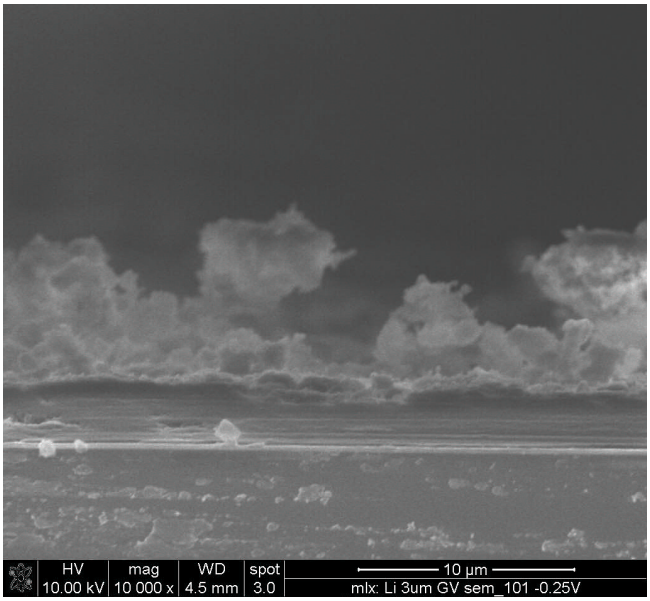

(b) Cross section

Figure 10: Lithium deposits made from $[Li(G1)_2][Tf_2N]$ on a copper wafer at a potential of $-0.25\,V$ vs. Li/Li^+. SEM pictures of the top view (a) and a cross section (b) are presented.

471, 486 and 508 eV and three KLL fluorine peaks around 608, 626 and 652 eV (Figure 11). For the detection of lithium, a statistically significant measurement was performed by measuring 3000 spectra which resulted in a high-resolution spectrum with a KLL lithium peak around 33 eV. The composition and relative atomic percentages of the various elements

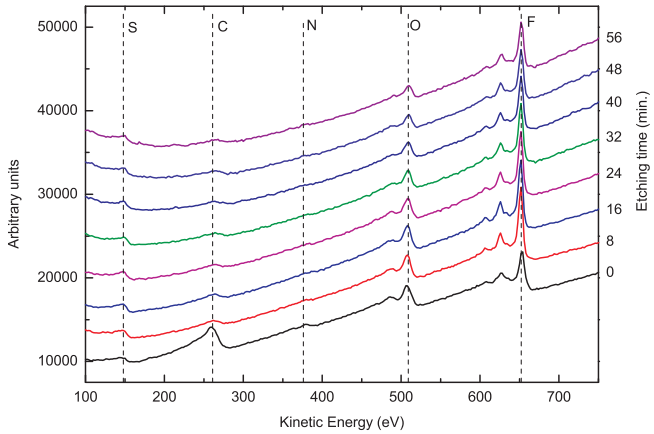

Figure 11: Overview of the Auger electron spectra of lithium deposits made from $[Li(G1)_2][Tf_2N]$ on a copper wafer at a potential of $-0.25\,V$ vs. Li/Li^+.

in the solid-electrolyte interface were calculated based on the peak area and sensitivity factor, with the "Thermo Scientific Avantage Data System" software (Figure 12). In the top layer, before etching a large amount of carbon species were detected from the decomposition of monoglyme. The carbon signal decreased rapidly with increasing etching time, indicating that only the top layer consists of decomposition products of the monoglyme ligands. This observation is in accordance with the results from the literature which indicate that the thickness the organic surface films formed on metallic lithium in ether electrolytes is of the order of 10 nm.[58,60] Next to carbon, a large percentage of nitrogen and fluorine compounds were detected and to a lesser extent oxygen and a small amount of sulfur species originating from the bis(trifluoromethylsulfonyl)imide anion. After eight min of sputtering, the nitrogen peak disappeared and the fluorine content increased dramatically, also sulfur and oxygen increased but to a lesser extent. Subsequent spectra with increasing etch time show less abrupt changes in composition, but it can be seen that the fluorine content increases steadily from the second spectrum (after 8 min of etching) until the final spectrum (after 56 min of sputtering), whereas the percentage of oxygen species remains approximately the same and sulfur compounds decrease with etching time.

From the etching experiment, it can be concluded that the solid-electrolyte interface mainly consists of decomposition products of the bis(trifluoromethylsulfonyl)imide anion,

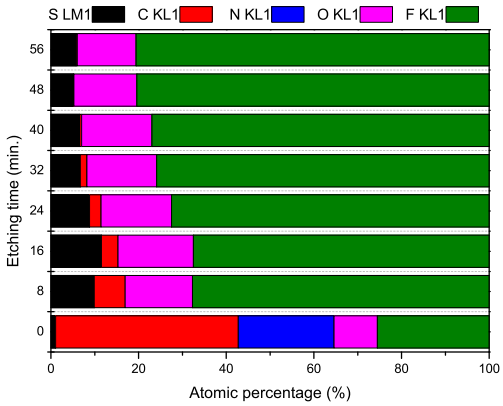

Figure 12: Overview of the relative atomic concentration of various elements during depth profiling of lithium deposits made from $[Li(G1)_2][Tf_2N]$ on a copper wafer at a potential of $-0.25\,V$ vs. Li/Li^+.

with a majority of fluorine-containing species and to a lesser extent oxygen and sulfur compounds. This is in accordance with earlier conclusions that the bis(trifluoromethylsulfonyl)imide anion has an important influence on the solid-electrolyte interface and thus the reversibility of the lithium deposition-stripping process.

Experimental

General methods

Melting points were determined using a Mettler-Toledo 822 DSC instrument at a heating rate of $5\,°C\ min^{-1}$ in a helium atmosphere. Aluminum crucibles were filled with 3–10 mg of the ionic liquid sample inside an argon-filled glove box and sealed to prevent contact with air. Viscosities were measured on a Brookfield cone plate viscometer (LVDV-II+ Programmable Viscometer) with a cone spindle CPE-40. The ionic liquid was kept under a dry nitrogen atmosphere during the measurement and the temperature of the sample was controlled by a circulating water bath. Single crystals of $[Li(G2)_2][I]$ were placed in a cold nitrogen stream of an Agilent Supernova diffractometer with Oxford Cryosystems cryostat operating at 100(2) K using Mo K α radiation (0.71073 Å) with the absorption correction applied using CrysAl-

isPro.[61] The structure was solved and refined using SHELXL.[62] The G2 ligand was found to be disordered and was modeled over two positions with the major disorder component found to comprise 68.4(3)% of the total. Restraints were required to keep the bond distances and thermal parameters in the two disorder components similar. Hydrogen atoms were placed in calculated positions and refined using the riding model. The OLEX2 program was used in the refinement and the creation of images.[63] CCDC 1005482 contains the supplementary crystallographic data for this paper and a view of the disorder with displacement ellipsoids and a packing plot can be found in the supplementary information. Lithium deposits were made on a copper wafer (Si/ 100 nm SiO_2/ 10 nm TaN/ 40 nm Ta/ 150 nm Cu), which was rinsed and dried three times with acetone and ethanol before use. After deposition the surface was rinsed with anhydrous 1,2-dimethoxyethane (Sigma-Aldrich) and dried using vacuum and argon purging. SEM imaging was performed using a FEI Nova200 nanoSEM or a Philips XL30 Field emission SEM using an electron beam with a voltage of 10 kV. Mass increase during deposition was measured using an electrochemical quartz crystal microbalance (Maxtek RQCM). A home-made cell was used to perform measurements with small quantities of electrolyte (approx. 5 mL), this cell was placed inside an argon-filled glove box with oxygen and water concentrations below 1 ppm. A copper substrate electrode on an AT-cut quartz crystal with a resonance frequency of 5 MHz was used as working electrode, platinum as counter electrode and silver as pseudo-reference electrode. Frequency changes were converted to mass changes in accordance with Sauerbrey's equation. Auger electron spectroscopy (AES) was used for elemental analysis of the solid-electrolyte interface (SEI). The Auger chamber (Thermo Scientific) was under ultra-high vacuum (8.9×10^{-9} torr) and spectra were measured using a primary electron beam with an energy of 8 keV with a typical current of 10 nA and a gaussian profile with a radius of about 0.5 mm. Auger electrons were detected with a hemispherical analyzer (Thermo Scientific) in an energy range from approx. 10 eV up to 800 eV. Depth profiling was done by sputtering with an argon ion beam for 8 min between each AES measurement up to 56 min of sputtering in total. The sputter beam

current was approx. 3 μA, the beam size had a Gaussian profile with a diameter of approx. 1 mm and was scanned over an area of 2×2 mm^2. For the sample transfer into the Auger chamber a home made transport chamber was built which could be loaded with the sample inside an argon-filled glove box with oxygen and water concentrations below 1 ppm. AES spectra were analyzed using Avantage Data System software (Thermo Scientific).

All electrochemical experiments were performed inside an argon-filled glove box with oxygen and water concentrations below 1 ppm. Cyclic voltammograms were measured in a three-electrode set-up, using lithium as counter and reference electrode, unless mentioned otherwise. A Solartron instruments SI 1287 , EG&G Princeton model 273 or EG&G Princeton model 263A were used as potentiostat, with Corrware software to control the electrochemical measurements. Working electrodes were polished, rinsed (with water, acetone and ethanol) and dried before each experiment. Electrolytes were not stirred during measurement.

Synthesis

All lithium-containing solvate ionic liquids were synthesized by the reaction between a lithium salt and a glyme ligand. Lithium salts, $LiTf_2N$ (IoLiTec), LiBr (Sigma-Aldrich) and LiI (Merck) were dried on a Schlenk line overnight at 100 °C. 1,2-Dimethoxyethane (G1) and 1-methoxy-2-(2-methoxyethoxy)ethane (G2) were purchased as anhydrous, 99.5% purity and used as received (Sigma-Aldrich). All dry reagents were stored in an argon-filled glove box with oxygen and water concentration less than 1 ppm. Ligands were added to the lithium salts in stoichiometric amounts and the mixture was stirred at elevated temperatures.

$[Li(G1)_x][Tf_2N]$ ($x = 1, 2, 3$). For the synthesis of $[Li(G1)_1][Tf_2N]$, G1 (0.317 g, 3.52 mmol) was added to $LiTf_2N$ (1.003 g, 3.49 mmol) and the mixture was stirred for 1 h at 50 °C. $[Li(G1)_2][Tf_2N]$ was formed by stirring a mixture of $LiTf_2N$ (1.002 g, 3.49 mmol) and G1 (0.630 g, 6.99 mmol) for 1 h at 50 °C. Finally $[Li(G1)_3][Tf_2N]$ was synthesized by stirring a mixture of $LiTf_2N$ (1.005 g, 3.50 mmol) with G1 (0.944 g, 10.5 mmol) for 1 h at a

temperature of 50 °C.

[Li(G2)$_x$][Tf$_2$N] (x = 2 [Li(G2)$_2$][Tf$_2$N] was prepared by adding G2 (0.935 g, 6.97 mmol) to LiTf$_2$N (1.001 g, 3.49 mmol) and stirring the mixture for 30 min at 100 °C.

[Li(G1)$_x$][Br] ($x = 2, 3$). [Li(G1)$_2$][Br] was formed by adding G1 (2.078 g, 23.1 mmol) to LiBr (1.001 g, 11.5 mmol) and stirring the solution for 30 min at 50 °C. [Li(G1)$_3$][Br] was prepared by stirring a mixture of G1 (1.560 g, 17.3 mmol) and LiBr (0.501 g, 5.77 mmol) for 1 h at a temperature of 70 °C.

[Li(G2)$_x$][Br] ($x = 1, 2$). [Li(G2)$_1$][Br] was synthesized by adding G2 (0.156 g, 1.16 mmol) to LiBr (0.101 g, 1.16 mmol) and stirring the mixture for 60 min. at 100 °C. However, this resulted in a very viscous liquid, even at high temperatures and was therefore not further investigated. [Li(G2)$_2$][Br] was formed by stirring a mixture of G2 (3.099 g, 23.1 mmol) and LiBr (1.002 g, 11.5 mmol) for 60 min at 100 °C.

[Li(G1)$_x$][I] ($x = 2, 3$). [Li(G1)$_2$][I] a mixture of G1 (1.347 g, 14.9 mmol) and LiI (1.005 g, 7.51 mmol) was stirred for 30 min at 75 °C. [Li(G1)$_3$][I] was synthesized by adding monoglyme (2.021 g, 22.4 mmol) to LiI (1.004 g, 7.50 mmol) and stirring the mixture for 30 min at 70 °C.

[Li(G2)$_x$][I] ($x = 1, 2$). [Li(G2)$_1$][I] was prepared by adding G2 (1.006 g, 7.50 mmol) to LiI (1.001 g, 7.48 mmol) and stirring the mixture for 60 min at 100 °C. However, this resulted in a very viscous liquid, which was not further investigated. To form [Li(G2)$_2$][I] a mixture of G2 (2.007 g, 15.0 mmol) and LiI (1.004 g, 7.50 mmol) was stirred for 30 min at 100 °C.

For $C_{12}H_{28}ILiO_6$ (M = 402.18 g mol^{-1}): orthorhombic, space group *Pccn* (no. 56), a = 10.1824(7) Å, b = 12.0243(8) Å, c = 14.6817(15) Å, V = 1797.6(3) Å^3, Z = 4, T = 100(2) K, μ(Mo Kα) = 1.799 mm^{-1}, D_{calc} = 1.486 g/cm^3, 11189 reflections measured (5.94° $\leq 2\Theta \leq$ 58.1°), 2196 unique (R_{int} = 0.0467, R_{sigma} = 0.0395) which were used in all calculations. The final R_1 was 0.0280 ($> 2\sigma(I)$) and wR_2 was 0.0607 (all data). Largest diff. peak/hole = 0.75/-0.38 e Å^3.

Conclusions

Various lithium-containing solvate ionic liquids were synthesized using a straightforward synthesis route consisting of a direct reaction between lithium salts and glyme ligands. Twelf different ionic liquids were synthesized, with the anions Tf_2N^-, Br^- or I^- and the ligands monoglyme or diglyme. The use of halides as anions in lithium-containing solvate ionic liquids resulted in a very low Coulombic efficiency of the reduction-oxidation cycles compared to solvate ionic liquids containing bis(trifluoromethylsulfonyl)imide. Two causes for this phenomenon are a poor solid-electrolyte interface formation or more extensive dendrite formation. The use of halide-containing solvate ionic liquids as electrolyte for lithium-ion batteries is not a good option because of the low anodic stability of halides compared with Tf_2N^- anions.

From cyclic voltammetry measurements it was concluded that high current densities were achievable without stirring the solution. However the reduction-oxidation process was not fully reversible, due to decomposition of the electrolyte and formation of a SEI. This was proven by EQCM and AES. Three different working electrodes were tested: copper, platinum and titanium, with platinum and copper giving the best efficiencies. Copper was eventually selected since it is a common current collector in lithium-ion batteries. Potentiostatic deposits of lithium from $[Li(G1)_2][Tf_2N]$ were made and investigated with SEM, which revealed a rough, but well covered surface.

Acknowledgement

The authors acknowledge financial support by the FWO-Flanders (research project research G.0B9613.N and research community "Ionic Liquids"), by the IWT-Flanders (SBO project IWT 80031 "MAPIL" and SBO project IWT 18142 "SoS-Lion") and by KU Leuven (project IDO/12/006 "IREBAT). We thank Sérgio Costa Miranda for his assistance with AES measurements and Marcel Lux for making the SEM images. Support by IoLiTec (Heilbronn,

Germany) is greatly appreciated. The authors also thank the Hercules Foundation for supporting the purchase of an X-ray diffractometer through project AKUL/09/0035.

Supporting Information Available

Characterization data of all compounds: ^{7}Li NMR, Raman spectra and ICP-OES analysis. XRD figures of $[Li(G2)_2][I]$: displacement ellipsoids and packing in the crystal structure.

This material is available free of charge via the Internet at `http://pubs.acs.org/`.

References

(1) MacFarlane, D. R.; Junhua, H. Lithium-Doped Plastic Crystal Electrolytes Exhibiting Fast Ion Conduction for Secondary Batteries. *Nature* **1999**, *402*, 792–794.

(2) Gray, F. M. An Interpretation of Raman Spectral Data for Polymer Electrolytes in the Light of New Evidence for Ion Association in Dilute-Solution. *J. Polym. Sci. Pol. Phys.* **1991**, *29*, 1441–1445.

(3) Welton, T. Room-Temperature Ionic Liquids. Solvents for Synthesis and Catalysis. *Chem. Rev.* **1999**, *99*, 2071–2084.

(4) Seddon, K. Ionic Liquids: A Taste of the Future. *Nat. Mater.* **2003**, *2*, 363–365.

(5) Plechkova, N. V.; Seddon, K. R. Applications of Ionic Liquids in the Chemical Industry. *Chem. Soc. Rev.* **2008**, *37*, 123–150.

(6) Navarra, M. Ionic Liquids as Safe Electrolyte Components for Li-metal and Li-Ion Batteries. *MRS Bull.* **2013**, *38*, 548–553.

(7) Basile, A.; Hollenkamp, A. F.; Bhatt, A. I.; O'Mullane, A. P. Extensive Charge-Discharge Cycling of Lithium Metal Electrodes Achieved Using Ionic Liquid Electrolytes. *Electrochem. Commun.* **2013**, *27*, 69–72.

(8) Bhatt, A. I.; Best, A. S.; Huang, J. H.; Hollenkamp, A. F. Application of the N-Propyl-N-Methyl-Pyrrolidinium Bis(fluorosulfonyl)imide RTIL Containing Lithium Bis(fluorosulfonyl)imide in Ionic Liquid Based Lithium Batteries. *J. Electrochem. Soc.* **2010**, *157*, A66–A74.

(9) Sano, H.; Sakaebe, H.; Matsumoto, H. Observation of Electrodeposited Lithium by Optical Microscope in Room Temperature Ionic Liquid-based Electrolyte. *J. Power Sources* **2011**, *196*, 6663–6669.

(10) Stark, J. K.; Ding, Y.; Kohl, P. A. Dendrite-Free Electrodeposition and Reoxidation of Lithium-Sodium Alloy for Metal-Anode Battery. *J. Electrochem. Soc.* **2011**, *158*, A1100–A1105.

(11) Budi, A.; Basile, A.; Opletal, G.; Hollenkamp, A.; Best, A. Study of the Initial Stage of Solid Electrolyte Interphase Formation upon Chemical Reaction of Lithium Metal and N-Methyl-N-Propyl-Pyrrolidinium-Bis(Fluorosulfonyl)Imide. *J. Phys. Chem. C* **2012**, *116*, 19789–19797.

(12) Howlett, P. C.; Brack, N.; Hollenkamp, A. F.; Forsyth, M.; MacFarlane, D. R. Characterization of the Lithium Surface in N-Methyl-N-Alkylpyrrolidinium Bis(trifluoromethanesulfonyl)amide Room-Temperature Ionic Liquid Electrolytes. *J. Electrochem. Soc.* **2006**, *153*, A595–A606.

(13) Markevich, E.; Sharabi, R.; Borgel, V.; Gottlieb, H.; Salitra, G.; Aurbach, D.; Semrau, G.; Schmidt, M. A. In Situ FTIR Study of the Decomposition of N-Butyl-N-Methylpyrrolidinium Bis(trifluoromethanesulfonyl)amide Ionic Liquid During Cathodic Polarization of Lithium and Graphite Electrodes. *Electrochim. Acta* **2010**, *55*, 2687–2696.

(14) Matsuda, Y.; Takemitsu, T.; Tanigawa, T.; Fukushima, T. Effect of Organic Additives in Electrolyte Solutions on Behavior of Lithium Metal Anode. *J. Power Sources* **2001**, *97–98*, 589–591.

(15) Aurbach, D.; Zinigrad, E.; Teller, H.; Cohen, Y.; Salitra, G.; Yamin, H.; Dan, P.; Elster, E. Attempts to Improve the Behavior of Li Electrodes in Rechargeable Lithium Batteries. *J. Electrochem. Soc.* **2002**, *149*, A1267–A1277.

(16) Mogi, R.; Inaba, M.; Jeong, S.-K.; Iriyama, Y.; Abe, T.; Ogumi, Z. Effects of Some Organic Additives on Lithium Deposition in Propylene Carbonate. *J. Electrochem. Soc.* **2002**, *149*, A1578–A1583.

(17) Sano, H.; Sakaebe, H.; Matsumoto, H. Effect of Organic Additives on Electrochemical Properties of Li Anode in Room Temperature Ionic Liquid. *J. Electrochem. Soc.* **2011**, *158*, A316–A321.

(18) Appetecchi, G.; Alessandrini, F.; Duan, R.; Arzu, A.; Passerini, S. Electrochemical Testing of Industrially Produced PEO-based Polymer Electrolytes. *J. Power Sources* **2001**, *101*, 42–46.

(19) Kuratomi, J.; Iguchi, T.; Bando, T.; Aihara, Y.; Ono, T.; Kuwana, K. Development of Solid Polymer Lithium Secondary Batteries. *J. Power Sources* **2001**, *97–98*, 801–803.

(20) Kwon, C. W.; Cheon, S. E.; Song, J. M.; Kim, H. T.; Kim, K. B.; Shin, C. B.; Kim, S. W. Characteristics of a Lithium-Polymer Battery Based on a Lithium Powder Anode. *J. Power Sources* **2001**, *93*, 145–150.

(21) Howlett, P. C.; MacFarlane, D. R.; Hollenkamp, A. F. High Lithium Metal Cycling Efficiency in a Room-Temperature Ionic Liquid. *Electrochem. Solid St.* **2004**, *7*, A97–A101.

(22) Ruther, T.; Huang, J.; Hollenkamp, A. F. A New Family of Ionic Liquids Based on N,N-Dialkyl-3-Azabicyclo[3.2.2]nonanium Cations: Organic Plastic Crystal Behaviour and Highly Reversible Lithium Metal Electrodeposition. *Chem. Commun.* **2007**, 5226–5228.

(23) Grande, L.; Paillard, E.; Kim, G.-T.; Monaco, S.; Passerini, S. Ionic Liquid Electrolytes for Li-Air Batteries: Lithium Metal Cycling. *Int. J. Mol. Sci.* **2014**, *15*, 8122–8137.

(24) Kim, G. T.; Jeong, S. S.; Xue, M. Z.; Balducci, A.; Winter, M.; Passerini, S.; Alessandrini, F.; Appetecchi, G. B. Development of Ionic Liquid-Based Lithium Battery Prototypes. *J. Power Sources* **2012**, *199*, 239–246.

(25) Marczewski, M. J.; Stanje, B.; Hanzu, I.; Wilkening, M.; Johansonn, P. "Ionic Liquids-in-Salt" – a Promising Electrolyte Concept for High–Temperature Lithium Batteries? *Phys. Chem. Chem. Phys.* **2014**, *16*, 12341–12349.

(26) Balbuena, P. B.; Wang, Y. *Lithium-Ion Batteries: Solid-Electrolyte Interphase*; Imperial college press: London, 2007.

(27) Brouillette, D.; Perron, G.; Desnoyers, J. Apparent Molar Volume, Heat Capacity, and Conductance of Lithium Bis(trifluoromethylsulfone)imide in Glymes and Other Aprotic Solvents. *J. Solution Chem.* **1998**, *27*, 151–182.

(28) Frech, R.; Huang, W. Conformational Changes in Diethylene Glycol Dimethyl Ether and Poly(ethylene oxide) Induced by Lithium Ion Complexation. *Macromolecules* **1995**, *28*, 1246–1251.

(29) Sutjianto, A.; Curtiss, L. A. Li-Diglyme Complexes: Barriers to Lithium Cation Migration. *J. Phys. Chem. A* **1998**, *102*, 968–974.

(30) Rhodes, C. P.; Frech, R. Local Structures in Crystalline and Amorphous Phases of Diglyme-$LiCF_3SO_3$ and Poly(ethylene oxide)$LiCF_3SO_3$ Systems: Implications for the Mechanism of Ionic Transport. *Macromolecules* **2001**, *34*, 2660–2666.

(31) Henderson, W. A.; McKenna, F.; Khan, M. A.; Brooks, N. R.; Young, V. G.; Frech, R. Glyme-Lithium Bis(trifluoromethanesulfonyl)imide and Glyme-Lithium Bis(perfluoroethanesulfonyl)imide Phase Behavior and Solvate Structures. *Chem. Mater.* **2005**, *17*, 2284–2289.

(32) Henderson, W. A. Glyme-Lithium Salt Phase Behavior. *J. Phys. Chem. B* **2006**, *110*, 13177–13183.

(33) Becker, G.; Eschbach, B.; Mundt, O.; Reti, M.; Niecke, E.; Issberner, K.; Nieger, M.; Thelen, V.; Nöth, H.; Waldhör, R. et al. Bis(1,2-Dimethoxyethan-O,O)Lithium-

Phosphanid, -Arsanid und -Chlorid Drei Neue Vertreter des Bis(1,2-Dimethoxyethan-O,O)Lithium-Bromid-Typs. *Z. Anorg. Allg. Chem.* **1998**, *624*, 469–482.

(34) Riffel, H.; Neumuller, B.; Fluck, E. Synthesis and Crystal-Structure of $[Li(DME)_2I]$. *Z. Anorg. Allg. Chem.* **1993**, *619*, 1682–1684.

(35) Choquette, Y.; Brisard, G.; Parent, M.; Brouillette, D.; Perron, G.; Desnoyers, J. E.; Armand, M.; Gravel, D.; Slougui, N. Sulfamides and Glymes as Aprotic Solvents for Lithium Batteries. *J. Electrochem. Soc.* **1998**, *145*, 3500–3507.

(36) Brouillette, D.; Irish, D. E.; Taylor, N. J.; Perron, G.; Odziemkowski, M. Stable Solvates in Solution of Lithium Bis(trifluoromethylsulfone)imide in Glymes and Other Aprotic Solvents: Phase Diagrams, Crystallography and Raman Spectroscopy. *Phys. Chem. Chem. Phys.* **2002**, *4*, 6063–6071.

(37) Ueno, K.; Yoshida, K.; Tsuchiya, M.; Tachikawa, N.; Dokko, K.; Watanabe, M. Glyme-Lithium Salt Equimolar Molten Mixtures: Concentrated Solutions or Solvate Ionic Liquids? *J. Phys. Chem. B* **2012**, *116*, 11323–11331.

(38) Angell, C. A.; Younes, A.; Zuofeng, Z. Ionic Liquids: Past, Present and Future. *Faraday Discuss.* **2012**, *154*, 9–27.

(39) Mandai, T.; Yoshida, K.; Ueno, K.; Dokko, K.; Watanabe, M. Criteria for Solvate Ionic Liquids. *Phys. Chem. Chem. Phys.* **2014**, *16*, 8761–8772.

(40) Tamura, T.; Hachida, T.; Yoshida, K.; Tachikawa, N.; Dokko, K.; Watanabe, M. New Glyme-Cyclic Imide Lithium Salt Complexes as Thermally Stable Electrolytes for Lithium Batteries. *J. Power Sources* **2010**, *195*, 6095–6100.

(41) Yoshida, K.; Tsuchiya, M.; Tachikawa, N.; Dokko, K.; Watanabe, M. Change from Glyme Solutions to Quasi-Ionic Liquids for Binary Mixtures Consisting of Lithium

Bis(trifluoromethanesulfonyl)amide and Glymes. *J. Phys. Chem. C* **2011**, *115*, 18384–18394.

(42) Seki, S.; Takei, K.; Miyashiro, H.; Watanabe, M. Physicochemical and Electrochemical Properties of Glyme-$LiN(SO_2F)_2$ Complex for Safe Lithium-ion Secondary Battery Electrolyte. *J. Electrochem. Soc.* **2011**, *158*, A769–A774.

(43) Zhang, C.; Ueno, K.-h.; Yamazaki, A.; Yoshida, K.; Moon, H.-j.; Mandai, T.; Umebaya shi, Y.-h.; Dokko, K.; Watanabe, M. Chelate Effects in Glyme/Lithium Bis(trifluoromethanesulfonyl)amide Solvate Ionic Liquids. I. Stability of Solvate Cations and Correlation with Electrolyte Properties. *J. Phys. Chem. B* **2014**, *118*, 5144–5153.

(44) Schaltin, S.; Brooks, N.; Binnemans, K.; Fransaer, J. Electrodeposition from Cationic Cuprous Organic Complexes: Ionic Liquids for High Current Density Electroplating. *J. Electrochem. Soc.* **2011**, *158*, D21–D27.

(45) Brooks, N. R.; Schaltin, S.; Van Hecke, K.; Van Meervelt, L.; Binnemans, K.; Fransaer, J. Copper(I)-Containing Ionic Liquids for High-Rate Electrodeposition. *Chem-Eur. J.* **2011**, *17*, 5054–5059.

(46) Schaltin, S.; Brooks, N. R.; Stappers, L.; Van Hecke, K.; Van Meervelt, L.; Binnemans, K.; Fransaer, J. High Current Density Electrodeposition from Silver Complex Ionic Liquids. *Phys. Chem. Chem. Phys.* **2012**, *14*, 1706–1715.

(47) Depuydt, D.; Brooks, N.; Schaltin, S.; Van Meervelt, L.; Fransaer, J. Silver-Containing Ionic Liquids with Alkylamine Ligands. *ChemPlusChem* **2013**, *78*, 578–588.

(48) Schaltin, S.; Brooks, N.; Sniekers, J.; Depuydt, D.; Van Meervelt, L.; Binnemans, K.; Fransaer, J. Room-Temperature Silver-Containing Liquid Metal Salts with Nitrate Anions. *Phys. Chem. Chem. Phys.* **2013**, *15*, 18934–18943.

(49) Sniekers, J.; Brooks, N. R.; Schaltin, S.; Van Meervelt, L.; Fransaer, J.; Binnemans, K. High Current Density Electrodeposition of Silver from Silver-Containing Liquid Metal Salts with Pyridine-N-Oxide Ligands. *Dalton Trans.* **2014**, *43*, 1589–1598.

(50) Edman, L. Ion Association and Ion Solvation Effects at the Crystalline-Amorphous Phase Transition in PEO-LiTFSI. *J. Phys. Chem. B* **2000**, *104*, 7254–7258.

(51) Rey, I.; Lassègues, J., J.C.and Grondin; Servant, L. Infrared and Raman Study of the PEO-LiTFSI Polymer Electrolyte. *Electrochim Acta* **1998**, *43*, 1505–1510.

(52) Rey, I.; Bruneel, J.; Grondin, J.; Servant, L.; Lassègues, J. Raman Spectroelectrochemistry of a Lithium/Polymer Electrolyte Symmetric Cell. *J. Electrochem. Soc.* **1998**, *145*, 3034–3042.

(53) Nowinski, J. L.; Lightfoot, P.; Bruce, P. G. Structure of $LiN(CF_3SO_2)_2$, a Novel Salt for Electrochemistry. *J. Mater. Chem.* **1994**, *4*, 1579–1580.

(54) Borgel, V.; Markevich, E.; Aurbach, D.; Semrau, G.; Schmidt, M. On the Application of Ionic Liquids for Rechargeable Li Batteries: High Voltage Systems. *J. Power Sources* **2009**, *189*, 331–336.

(55) Yan, B.; Yang, P.; Zhao, Y.; Zhang, J.; An, M. Electrocodeposition of Lithium and Copper from Room Temperature Ionic Liquid 1-Ethyl-3-Methylimidazolium Bis(trifluoromethylsulfonyl)imide. *R. Soc. Chem. Adv.* **2012**, *2*, 12926–12931.

(56) Lewandowski, A.; Biegun, M.; Galinski, M. Kinetics of Li^+ Reduction in 1-Methyl-3-Propylpiperidinium Bis(trifluoromethylsulfonyl) Imide Room Temperature Ionic Liquid. *Electrochim. Acta* **2012**, *63*, 204–208.

(57) Bard, A. J.; Inzelt, G.; Scholz, F. *Electrochemical Dictionary*; Springer-Verlag Berlin Heidelberg: Berlin, 2008.

(58) Aurbach, D.; Daroux, M.; McDougall, G.; Yeager, E. B. Spectroscopic Studies of Lithium in an Ultrahigh Vacuum System. *J. Electroanal. Chem.* **1993**, *358*, 63–76.

(59) Serizawa, N.; Seki, S.; Takei, K.; Miyashiro, H.; Yoshida, K.; Ueno, K.; Tachikawa, N.; Dokko, K.; Katayama, Y.; Watanabe, M. et al. EQCM Measurement of Deposition and Dissolution of Lithium in Glyme-Li Salt Molten Complex. *J. Electrochem. Soc.* **2013**, *160*, A1529–A1533.

(60) Peled, E. Film Forming Reaction at the Lithium/Electrolyte Interface. *J. Power Sources* **1983**, *9*, 253–266.

(61) CrysAlisPro, Agilent Technologies, Yarnton, UK. **2011**,

(62) Sheldrick, G. M. A Short History of SHELXL. *Acta Cryst. A* **2008**, *64*, 112–122.

(63) Dolomanov, O. V.; Bourhis, L. J.; Gildea, R. J.; Howard, J. A. K.; Puschmann, H. OLEX2: a Complete Structure Solution, Refinement and Analysis Program. *J. Appl. Cryst.* **2009**, *42*, 339–341.

Graphical TOC Entry